ARCHIVES OF ELECTRICAL ENGINEERING VOL. 72(3), pp. 715–735 (2023)

DOI 10.24425/aee.2023.146046

Influence of the converter transformer valve-side bushing fault on commutation reactance protection and improvement scheme

YANXIA ZHANG ✉, GUANGHAO DONG, LE WEI, JINTING MA, SHANSHAN DU

School of Electrical and Information Engineering, Tianjin University
No. 92 Weijin Road, Nankai District, Tianjin, China
e-mail: {✉zyx1962/dss1998}@tju.edu.cn, {dong_guanghao/15227039236/15822957005}@163.com

(Received: 25.01.2023, revised: 18.04.2023)

Abstract: Commutation reactance is an important component in the voltage-source converter-based high-voltage direct current (VSC–HVDC) transmission system. Due to its connection to the converter, when there is a fault occurring on the valve-side bushing of a converter transformer, the nonlinearity operation of the converter complicates the characteristics of current flowing through commutation reactance, which may lead to maloperation of its overcurrent protection. It is of great significance to study the performance of commutation reactance overcurrent protection under this fault condition and propose corresponding improvement measures to ensure the safe and stable operation of AC and DC systems. In the VSC–HVDC system with the pseudo-bipolar structure of a three-phase two-level voltage source converter, the valve has six working periods in a power frequency cycle, and each period is divided into five working states. According to the difference between the fault phase and non-fault phase of the conductive bridge arms at the time of fault occurrence, these five working states are merged into two categories. On this basis, various faults of the valve-side bushing of a converter transformer are analyzed, and the conclusion is drawn that the asymmetric fault of valve-side bushing can lead to the maloperation of the commutation reactance overcurrent protection. Based on the characteristics that the current flowing through the commutation reactance after the asymmetric fault of the valve-side bushing contains decaying aperiodic components in addition to the fundamental frequency wave, a scheme to prevent the maloperation of commutation reactance overcurrent protection is proposed, which uses the unequal of two half cycle integral values with different starting points to realize the blocking of commutation reactance overcurrent protection, and it makes up the deficiency of existing protection in this aspect. Finally, this paper builds a VSC–HVDC system simulation model in the PSCAD/EMTDC platform to verify the effectiveness of the scheme.

Key words: commutation reactance, converter transformer, improvement scheme, overcurrent protection, valve-side bushing fault, VSC–HVDC system

1. Introduction

Voltage-source converter-based high-voltage direct current (VSC–HVDC) transmission which is called flexible high-voltage direct-current transmission has the advantages of fast control of active and reactive power and being connected with the weak AC network or even passive network [1–3]. Currently, it has mainly three topological structures: two-level converters, diode clamp three-level converters, and modular multilevel converters (MMC) [4–6]. Commutation reactance as the key component of the flexible DC transmission system, together with the converter transformer, forms the link of energy exchange of the AC/DC interconnected system, with the functions of isolating the AC power grid and voltage-source converter, restraining harmonic current, completing energy storage and transmission, which is crucial to AC/DC systems. Therefore, the analysis of the protection performance of commutation reactance and the research on a new protection principle of commutation reactance play a significant role in prolonging the service life of commutation reactance and ensuring the safe and stable operation of AC/DC systems.

At present, commutation reactance is equipped with overcurrent protection. However, on the one hand, since commutation reactance is directly connected with the converter, the nonlinearity of the converter operation makes the fault characteristics of commutation reactance complicated; on the other hand, the overcurrent protection of commutation reactance is not equipped with a directional element, so there is a risk of misoperation of the converter transformer valve-side bushing fault. Therefore, aiming at the valve-side bushing fault of the converter transformer, this paper carries out research on its influence on commutation reactance overcurrent protection and the improved scheme, and firstly the valve-side bushing fault needs to be analyzed. In the existing literature, reference [7] establishes the zero-sequence equivalent circuit after the single-phase grounding fault of the converter transformer valve-side bushing in the VSC–HVDC system, analyzes the flow path of the zero-sequence current, and derives the expression of the capacitor voltage on the DC side. However, the expression of the bushing current on the valve side is not derived. Reference [8] establishes the equivalent circuits of the asymmetrical fault of the converter transformer valve-side bushing and DC line single-pole grounding fault under different grounding modes of the DC side capacitor midpoint, and qualitatively analyzes the characteristics of the valve-side bushing current. The disadvantage is that the analysis process depends on the simulation results, and there is a gap with the actual situation. References [9] and [10] analyze the zero-sequence current flow paths of the single-phase grounding fault of the converter transformer valve-side bushing in the VSC–HVDC system, deduce the expression of the zero-sequence impedance, and point out that the zero-sequence impedance and the system commutation reactance cancel each other, resulting in a small total impedance and a large bushing current. But other types of faults on the valve-side bushing are not analyzed. Reference [11] verifies the conclusions of [9] and [10] through simulations. On the basis of establishing the equivalent circuit of the single-phase grounding fault of the converter transformer valve-side bushing in the VSC–HVDC system, reference [12] deduces the expressions of the three-phase current of the bushing and obtains the following variation rules: after the converter is locked, the fault phase

current has better sinusoidal characteristics, while the non-fault phase current is equal to 0 for about 1/2 of the period, greater than 0 for 1/4 of the period, and less than 0 for 1/4 of the period. Based on the variation characteristics, a method for identifying the fault type and the location is proposed. Reference [13] analyzes the currents transient characteristics before and after the converter is locked in case of the valve-side bushing fault of the converter transformer in the VSC–HVDC system, and points out that the current flowing through the bushing is the capacitor discharge current, which is the oscillation attenuation component. The deficiency lies in the lack of research on commutation reactance protection.

From the above analysis, it can be seen that current studies on valve-side bushing faults mainly focus on single-phase grounding faults, and there is no qualitative analysis of the bushing fault current, as well as literature to study the influence of valve-side bushing faults of the converter transformer on commutation reactance protection. This paper summarizes the six working periods of a power frequency period in the VSC–HVDC system into five working states, divides five working states into two working types according to the difference between the fault phase and the non-fault phase of the conductive bridge arms after a bushing fault occurs on the converter transformer valve side, and analyzes the current components flowing through the commutation reactance current transformer and the influence on the overcurrent protection after the valve-side bushing faults of the converter transformer. Based on the characteristics that there are decaying aperiodic components in the current flowing through the commutation reactance, this paper proposes a scheme to prevent the maloperation of the commutation reactance overcurrent protection, and builds the simulation model to verify the effectiveness of the scheme. The organization of the paper is as follows: in Section 2, each working period of the valve is divided into five working states in the VSC–HVDC system with a pseudo-bipolar structure of a three-phase two-level voltage source converter, and according to the difference between the fault phase and the non-fault phase of the conductive bridge arms at the time of fault occurrence, the five working states are merged into two categories. On this basis, the influence of different types of short-circuit faults occurring on the valve-side bushing of the converter transformer on commutation reactance overcurrent protection is analyzed, and it points out that the asymmetric fault of the valve-side bushing can lead to the maloperation of commutation reactance overcurrent protection. In Section 3, based on the characteristics that the current flowing through the commutation reactance current transformer after the asymmetric fault of the valve-side bushing contains decaying aperiodic components, a scheme to prevent the maloperation of commutation reactance overcurrent protection is proposed. In Section 4, the VSC–HVDC system simulation model is built on the PSCAD/EMTDC platform to verify the effectiveness of the scheme. Section 5 is the conclusion of this paper.

2. Influence of converter transformer valve-side bushing fault on commutation reactance overcurrent protection

2.1. Three-phase short circuit of the valve-side bushing

Figure 1 shows the VSC–HVDC system of the three-phase two-level voltage source converter widely used in practical engineering [14–16].

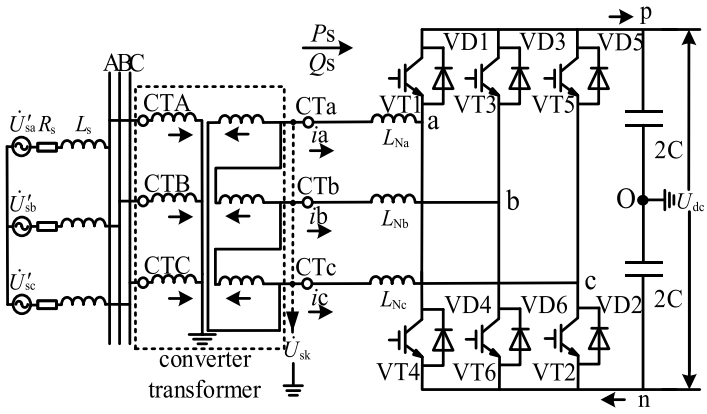

Fig. 1. Sending topological structure of three-phase two-level VSC–HVDC system

The commutation reactance L_{Na} has the functions of isolating the AC grid from the converter, storing and transmitting energy. The midpoint of the DC side capacitor is grounded. Each phase of the three-phase two-level voltage source converter consists of upper and lower bridge arms, and each bridge arm includes a group of insulated gate bipolar transistors and its anti-parallel freewheeling diode; $\dot{U}'_{sa}$, $\dot{U}'_{sb}$, $\dot{U}'_{sc}$ and $\dot{U}_{sa}$, $\dot{U}_{sb}$, $\dot{U}_{sc}$ are the three-phase voltages of the AC equivalent system and the valve side of the converter transformer, respectively; R_S and L_S are the resistance and inductance of the AC equivalent system; The converter transformer adopts a YN/Δ wiring connection; CTA, CTB, CTC and CTa, CTb, CTc are the three-phase current transformers on the grid-side and valve-side bushings of the converter transformer; i_a, i_b and i_c are the currents of CTa, CTb, CTc, respectively, and the positive direction of the specified current is shown in Fig. 1.

The sinusoidal pulse width modulation (SPWM) in PWM modulation techniques to control the on-off state of the converter valve is mostly adopted in engineering [17]. As shown in Fig. 2, according to the zero-crossing point of the three-phase voltages on the valve side, a power

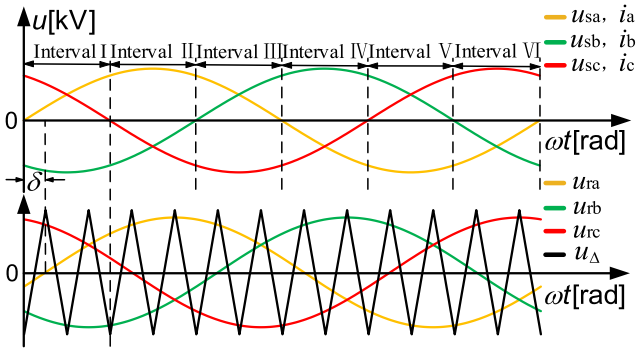

Fig. 2. Modulated signal waveforms and interval division of VSC converter valve

frequency period is divided into six intervals from I to VI at 60° intervals, in each interval, two phase voltages have the same sign, while the other phase voltage has the opposite sign.

The three-phase modulated waves (u_{ra}, u_{rb}, u_{rc}) lagging behind the valve-side voltage of angle δ are compared with the triangular carrier wave (u_Δ) with frequency N times of modulated waves: when the amplitudes of the modulated waves are greater than the carrier wave, the valve receives the conduction signal of the upper bridge arm; otherwise it receives the conduction signal of the lower bridge arm. Whether the IGBT or diode is on in the bridge arm depends on the positive or negative voltage at both ends of the bridge arm.

Each interval can be divided into multiple time periods according to the relationship between the three-phase modulated waves and the triangular carrier wave. Figure 3 shows the 13 time periods of interval I ($u_{sa} > 0$, $u_{sb} > 0$, $u_{sc} > 0$) when the carrier ratio $N = 12$ and Table 1 gives the corresponding switching sequence of elements.

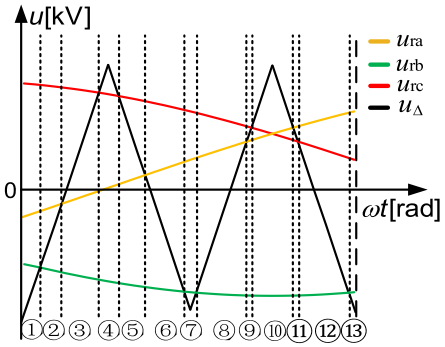

Fig. 3. Time period division of interval I

In Table 1, "1" in the modulated signal indicates that the upper half bridge arm is on, and "0" indicates that the lower half bridge arm is on. As shown in Table 1:

1. At any time period, there are always three elements on in the converter valve;
2. Although there are 13 kinds of modulated signals in interval I, they can be classified into 5 categories: [000], [001], [100], [101] and [111].

As the triangular carrier ratio N increases, the time periods in interval I increases, but the class of modulated signal remains unchanged. The other intervals are the same.

Assuming that the valve-side bushing three-phase short-circuit occurs when the modulated signal is [101], the voltage at the fault point drops to 0, and VD1, VD5, and VD6, which had been on before the fault, are off due to withstanding the reverse voltage after the short circuit. The fault current flow paths on the valve side of the converter transformer is shown in Fig. 4, where E_{eq} and R_{eq} are the equivalent electric potential and resistance of the DC system [18]. There are three flow paths: ① Part of the discharge current of the positive electrode capacitor flows to the fault point through VT1, the commutation reactance L_{Na}, and the rest enters the ground through the DC positive electrode; ② The current at the fault point flows through L_{Nb} of phase b and the conducting VT6 to point n, and then enters the ground through the negative electrode capacitor after merging with the DC negative current; ③ The current supplied by the AC equivalent system flows into the valve-side winding.

Table 1. Switching sequence of elements in interval I

Period	**Modulated signal**	**Conduction elements (i = 1 ~ 6)**					
		VTi			VDi		
①	[111]		3		1		5
②	[101]				1	6	5
③	[001]	4				6	5
④	[000]	4		2		6	
⑤	[001]	4				6	5
⑥	[101]				1	6	5
⑦	[111]		3		1		5
⑧	[101]				1	6	5
⑨	[001]	4				6	5
⑩	[000]	4		2		6	
⑪	[100]			2	1	6	
⑫	[101]				1	6	5
⑬	[111]		3		1		5

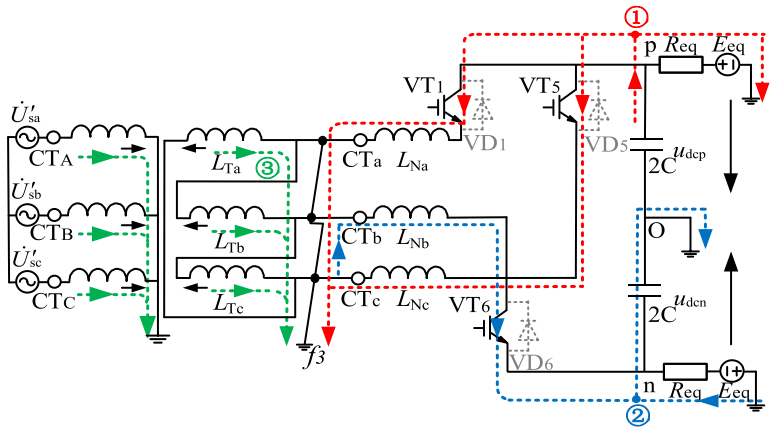

Fig. 4. Current paths of three-phase short circuit fault under [101] modulated status

The currents flowing through CTa and CTc are the positive electrode capacitor discharge current, which are the decaying aperiodic components gradually decaying to 0; the current flowing through CTb is the negative electrode capacitor discharge current, which is also the

decaying aperiodic component that gradually decays to 0. Therefore, the overcurrent protection of commutation reactance that reflects the fundamental frequency component will not misoperate. In the case of other modulated signals, the fault current flow circuit of the three-phase short circuit is similar, and the protection will not misoperate.

2.2. Single-phase short circuit of the valve-side bushing

Case 1: The conducting bridge arms of fault phase and non-fault phase are different

The modulated signals [001], [100], and [101] all belong to this kind of situation, and the modulated state [101] is taken as an example to analyze. After the *a*-phase valve-side bushing is grounded, the *a*-phase voltage drops to 0 and VD1 shuts off withstanding the reverse voltage. Figure 5 shows the current flow paths after the fault: ① Part of the discharge current of the positive electrode capacitor flows to the fault point through VT1 and L_{Na}, and the rest enters the ground through the DC positive electrode; ② The short-circuit current supplied by the AC equivalent system flows into the valve-side winding.

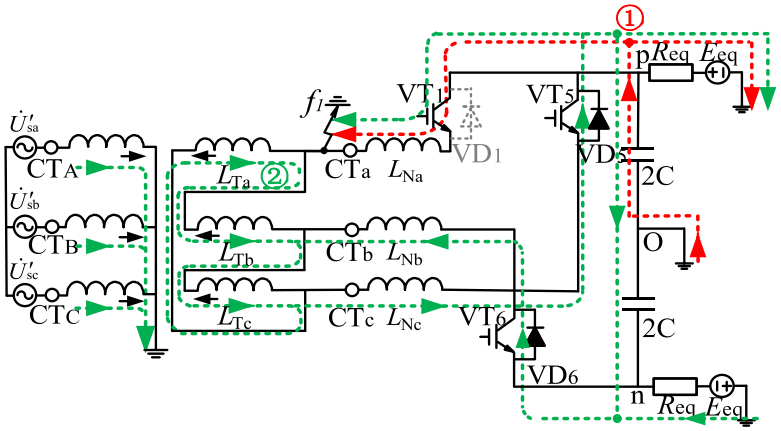

Fig. 5. A-phase valve-side bushing is grounded when the conducting bridge arms of fault phase and non-fault phase are different

In this state, the positive electrode capacitor discharge current only flows through CTa, and gradually decays to 0. Part of *c*-phase current forms a loop through VD5, the DC side and *b*-phase, and the rest flows to the fault point through VD5 and VT1. Therefore, the current of CTa includes two parts: one is the capacitor discharge current, and the other is the fundamental frequency current; the currents flowing through CTb and CTc are all the fundamental frequency current.

Due to the existence of the fault point, AC circuit impedance decreases, and the fundamental frequency currents flowing through CTa, CTb, and CTc are far bigger than that under normal operation, so the three-phase overcurrent protection will misoperate.

Case 2: The conducting bridge arms of fault-phase and non-fault phase are the same

Such cases include modulated signals [000] and [111], and the modulated state of [111] is taken as an example to analyze. After the *a*-phase valve-side bushing is grounded, the current

flow path on the valve side of the converter transformer is shown in Fig. 6. One part of the current of loop ① flows to the fault point through VT1, L_{Na} or VT3, L_{Nb}, b-phase reactance L_{Tb} of the converter transformer, and the other part enters the ground through the DC positive electrode; Loop ② is formed by the negative electrode capacitor and the DC negative electrode because the lower bridge arm has not a conducting converter valve; Loop ③ is the short-circuit current supplied by the AC equivalent system.

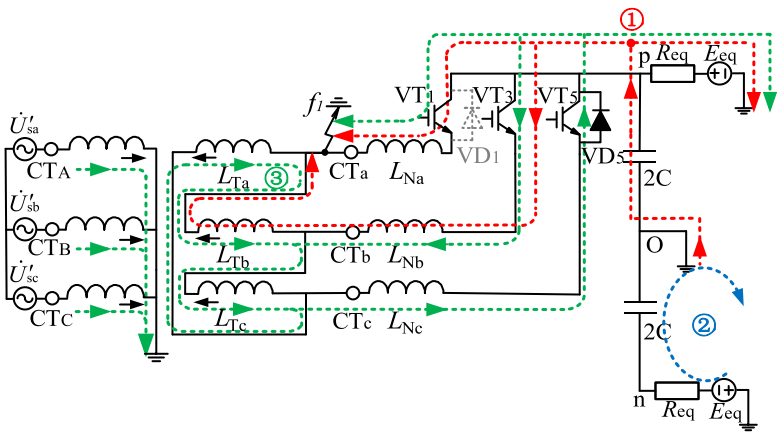

Fig. 6. A-phase valve-side bushing is grounded when the conducting bridge arms of fault-phase and non-fault phase are the same

The positive electrode capacitor discharge current flows through L_{Na}, L_{Nb}, CTa and CTb, and it gradually decays to 0. Part of the c-phase current flows through the DC side to form a loop, and the rest flows to the fault point through VD5, VT1 or VT3, respectively. The currents flowing through CTa and CTb include capacitor discharge current and fundamental frequency current, while the current of CTc is only the fundamental frequency one. Similarly to case 1, the existence of the fault point reduces AC circuit impedance, making the fundamental frequency current flowing through CTa, CTb and CTc far bigger than that under normal operation, so the three-phase overcurrent protection will misoperate.

2.3. Two-phase short circuit of the valve-side bushing

Case 1: The conducting bridge arms of fault-phase and non-fault phase are different

Under the [101] modulated signal state, when the a-phase-to-b-phase valve-side bushing short circuit occurs on the valve-side bushing, the voltage at the fault point decreases, and VD1 and VD6, which were on before the fault, are off under reverse voltage. There are three current flow paths as shown in Fig. 7: ① Part of the discharge current of the positive electrode capacitor flows to the fault point through VT1 and L_{Na}, and then it flows through L_{Nb}, VT6 and enters the ground after merging with the negative electrode capacitor discharge current. The rest enters the ground through the DC positive electrode; ② The short-circuit current supplied by the AC equivalent system; ③ The circulating current is formed by the induced voltage of the b-phase winding.

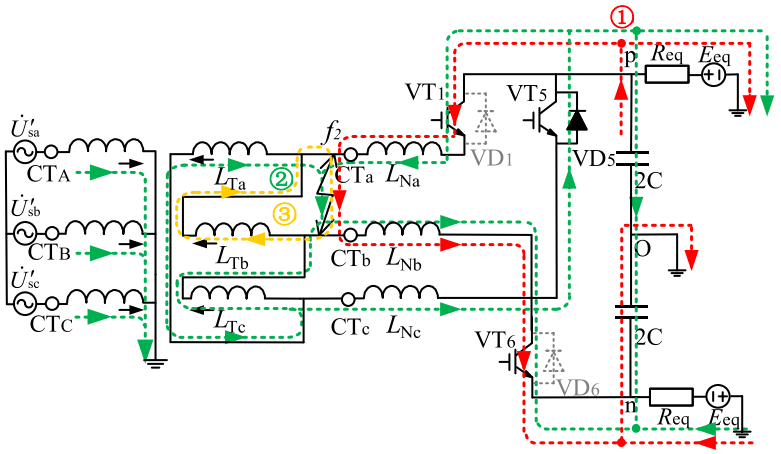

Fig. 7. Two-phase bushing short circuit when the conducting bridge arms of fault phase and non-fault phase are different

The positive electrode capacitor discharge current flows through CTa and CTb, and gradually decays to 0. Part of the *c*-phase current flows to the DC side, and the rest flows to the fault point through VD5 and VT1. Therefore, the currents of CTa and CTb include capacitor discharge current and fundamental frequency current, while the current of CTc is only the fundamental frequency one. Similar to the single-phase grounding of the valve-side bushing, the three-phase overcurrent protection will misoperate.

Case 2: The conducting bridge arms of fault phase and non-fault phase are the same

The current flow paths of *a*-phase-to-*b*-phase valve-side bushing short circuit under the [111] modulated signal state is shown in Fig. 8: ① Part of the discharge current of positive electrode

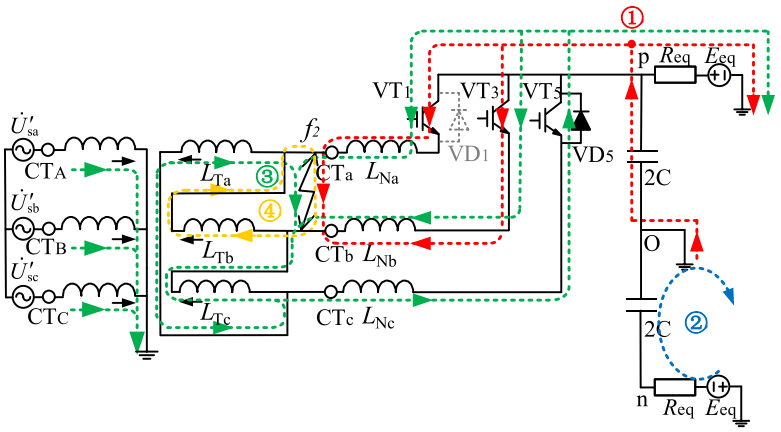

Fig. 8. Two-phase *b*ushing short circuit when the conducting bridge arms of fault phase and non-fault phase are the same

capacitor flows to the fault point through VT1, L_{Na} and VT3, L_{Nb}, and the rest enters the ground through the DC positive electrode; ② The negative electrode capacitor forms a loop with the DC negative electrode due to the lower bridge arm has not a conducting converter valve; ③ The short-circuit current supplied by the AC equivalent system; ④ The circulating current is formed by the induced voltage of the *b*-phase winding.

It can be seen from Fig. 8 that the positive electrode capacitor discharge current flows through L_{Na}, L_{Nb} and CTa, CTb, and gradually decays to 0. Part of *c*-phase current forms a loop through the DC side, and the rest flows to the fault point through VD5, VT1 or VT3 respectively. The fundamental frequency currents of CTa, CTb and CTc are far bigger than that under normal operation, so the three-phase overcurrent protection will misoperate.

2.4. Two-phase short-circuit grounding of the valve-side bushing

Case 1: The conducting bridge arms of fault-phase and non-fault phase are different

Assuming that two-phase valve-side bushing grounding of *a*-phase and *b*-phase occurs when the modulated signal is [101], the voltage at the fault point drops to 0, and VD1, VD6, which were on before the fault, are off under the reverse voltage. There are four current flow paths in Fig. 9: ① Part of the discharge current of positive electrode capacitor flows to the fault point through VT1, L_{Na}, and the rest enters the ground through the DC positive electrode; ② The current at the fault point flows through L_{Nb}, VT6 to point *n*, and then enters the ground after merging with the negative electrode capacitor discharge current; ③ The short-circuit current supplied by the AC equivalent system flows into the valve-side winding; ④ The circulating current is formed by the induced voltage of the *b*-phase winding.

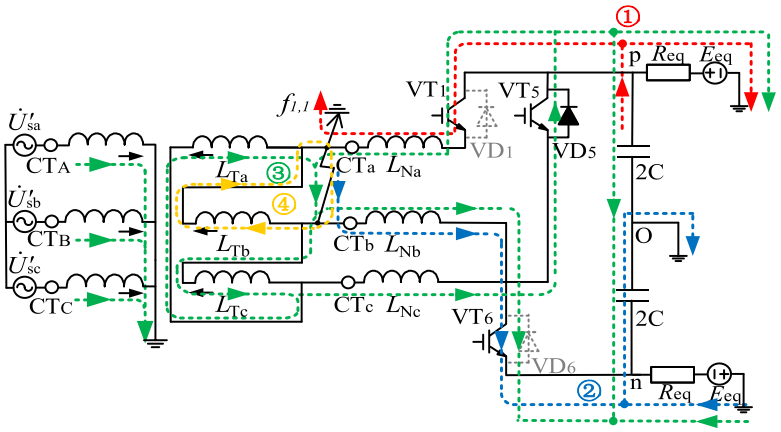

Fig. 9. Two-phase valve-side bushing grounding of *a*-phase and *b*-phase when the conducting bridge arms of fault phase and non-fault phase are different

Similar to the two-phase short circuit, the current flowing through CTa is the positive electrode capacitor discharge current, while the current flowing through CTb is the negative electrode capacitor discharge current gradually decaying to 0. Part of *c*-phase current flows to the DC side, and the rest flows to the fault point through VD5, VT1. The currents of CTa, CTb include

capacitor discharge current and fundamental frequency current, and that of CTc is fundamental frequency one. The three-phase overcurrent protection will misoperate.

Case 2: The conducting bridge arms of fault phase and non-fault phase are the same

Under the [111] modulated signal state, the VD1, which was on before the fault, is off due to the reverse voltage, and there are four current flow paths as shown in Fig. 10: ① Part of the discharge current of positive electrode capacitor flows to the fault point through VT1, L_{Na} or VT3, L_{Nb}, and the rest enters the ground through the DC positive electrode; ② The negative electrode capacitor forms a loop with the DC negative electrode due to the lower bridge arm has not a conducting converter valve; ③ The short-circuit current supplied by the AC equivalent system flows into the valve-side winding; ④ The circulating current is formed by the induced voltage of the *b*-phase winding.

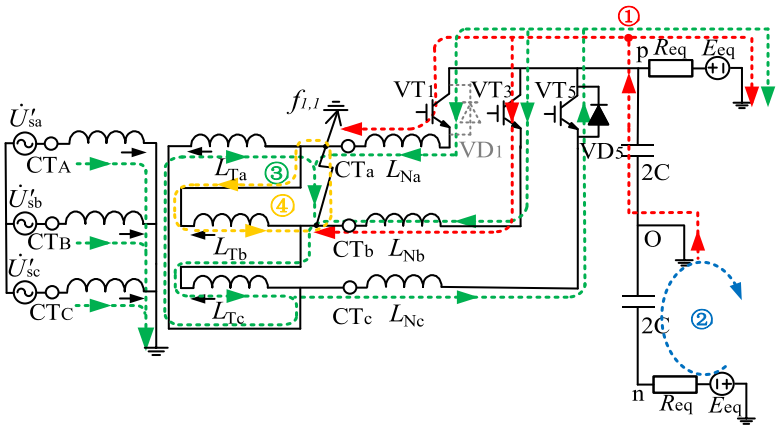

Fig. 10. Two-phase valve-side bushing grounding of *a*-phase and *b*-phase when the conducting bridge arms of fault phase and non-fault phase are the same

The positive electrode capacitor discharge current flows through CTa, CTb and gradually decays to 0; part of *c*-phase current forms a loop through the DC side and the rest flows to the fault point through VD5, VT1 or VT3, respectively. The currents of CTa, CTb also include capacitor discharge current and fundamental frequency current, and that of CTc is fundamental frequency current. The existence of the fault point reduces the AC circuit impedance, and the fundamental frequency currents of CTa, CTb and CTc are far bigger than that under normal operation, so the three-phase overcurrent protection will misoperate.

3. A scheme to prevent maloperation of commutation reactance overcurrent protection

The valve-side bushing fault of the converter transformer belongs to the out-of-area fault of commutation reactance, the overcurrent protection of commutation reactance should not operate. However, based on the above analysis, it can be seen that various asymmetric faults on the valve-

side bushing will cause the overcurrent protection to misoperate. Therefore, it is necessary to study the blocking scheme to prevent the misoperation.

By summarizing the above analysis results, it can be concluded that the common characteristics of asymmetrical faults occurs on the valve-side bushing are as follows: the CT current of the fault phase commutation reactance contains the decaying aperiodic component in addition to the fundamental frequency component. Based on this characteristic, this paper proposes the following blocking scheme for overcurrent protection.

The half-cycle absolute value integration is carried out for the current of commutation reactance after a fault to obtain the integral value S. Because the current contains the decaying aperiodic component after an asymmetrical fault occurs on the valve-side bushing, the integral values of two different half-cycles are not equal. So, the criterion of the blocking scheme is

$$\left|S_{\text{full current}(t_1)} - S_{\text{full current}(t_2)}\right| > S_{\text{set}} \quad \text{Lasts for 3 ms,} \tag{1}$$

where: $S_{\text{full current}(t_1)}$ and $S_{\text{full current}(t_2)}$ are the integral values of the half-cycle absolute value of commutation reactance current starting from t_1 and t_2, respectively. t_1 is the time when the fault occurs, and t_2 is 3 ms after the fault occurs. Theoretically, the setting value S_{set} can be taken as 0 because the system does not contain the decaying aperiodic component under normal operating conditions and after a fault in a steady state. In practice, S_{set} is set by 10% of the half-cycle integral value of fundamental current under normal operation. If this criterion is satisfied for 3 ms, the overcurrent protection will be blocked.

The following analyzes the action performance of the blocking criterion in Eq. (1) in the internal fault of commutation reactance. Internal fault is divided into two cases according to whether CT flows through the decaying aperiodic component. For the first case, take the single-phase grounding when the modulated signal in Fig. 11 is [101] as an example. According to the flow paths of the fault current, the currents of CTa, CTb and CTc do not contain a decaying aperiodic component, so the blocking criterion is not satisfied, and the fault is removed because the overcurrent protection is not blocked. This paper analyzes the asymmetric faults of commutation

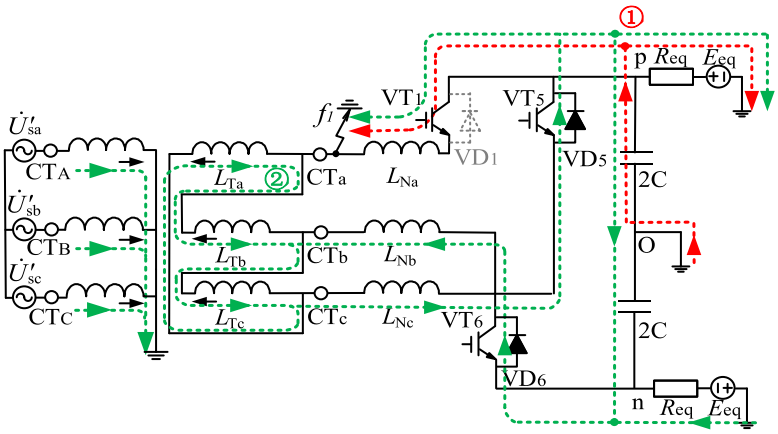

Fig. 11. The decaying aperiodic component does not flow through the CT

reactance under other modulated signals and finds that most of them belong to this situation, that is, the blocking criterion does not act, as shown in detail in Table 2.

Table 2. CT current component of commutation reactance fault

Fault type	**State**	**Internal fault of commutation reactance**		
		Whether CTa has the decaying aperiodic component	**Whether CTb has the decaying aperiodic component**	**Whether CTc has the decaying aperiodic component**
Single-phase grounding	Case 1	No	No	No
	Case 2	Yes	Yes	No
Two-phase short circuit	Case 1	No	No	No
Two-phase grounding	Case 1	No	No	No

The second case only includes the single-phase grounding under modulated signal [111]. Figure 12 shows the current flow paths. The currents of CTa, CTb contain a decaying aperiodic component, which is also listed in Table 2. However, in this case, because the fault current flows through the valve side impedance of the converter transformer, its value is reduced, so the half-cycle integral difference is less than the setting value S_{set}, the blocking criterion is not satisfied, and the fault is removed because the overcurrent protection is not blocked.

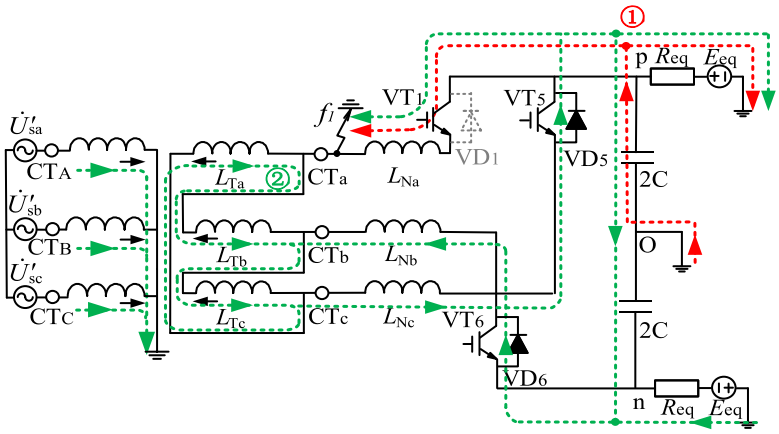

Fig. 12. The decaying aperiodic component flows through the CT

According to the above analysis, the blocking criterion in this paper has the clear selectivity and can be reliably blocked when an asymmetric fault occurs on the valve-side bushing of the converter transformer. The commutation reactance overcurrent protection with blocking criteria is shown in Fig. 13.

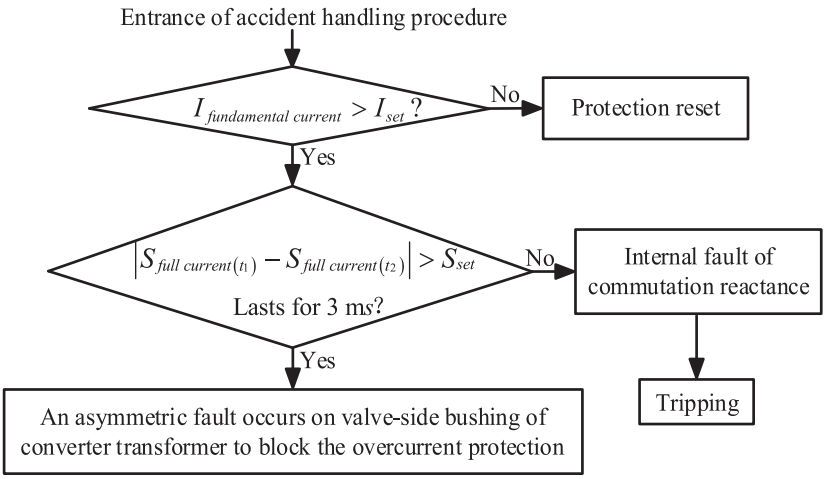

Fig. 13. The commutation reactance overcurrent protection flowchart with blocking criterion

4. Simulation

The VSC–HVDC system simulation model built by PSCAD/EMTDC is shown in Fig. 14. The rectifier side adopts constant active and constant reactive power control and the inverter side adopts constant DC voltage and constant reactive power control [19]. The simulation model parameters are listed in Table 3. The fault occurrence time is set at 2 s, and the simulation sampling frequency is 2 kHz.

Table 3. The main parameters of simulation model system

Parameters	**The values of the rectifier side**	**The values of the rectifier side**
AC rated voltage at grid side/ [kV]	220	110
Rated capacity of the converter transformer/ [MVA]	200	200
Transformation ratio of the converter transformer	230 kV/345 kV	330 kV/121 kV
DC side capacitance/ [μF]	150	150
Commutation reactance/ [mH]	10	10

The three-phase current during normal operation is shown in Fig. 15.
The half-cycle integral value of the fundamental frequency current is

$$S_{\text{fundamental current}} = 3.015\ \text{A} \cdot \text{s}.$$

Therefore, the setting value is selected as

$$S_{\text{set}} = 10\% S_{\text{fundamental current}} = 0.301\ \text{A} \cdot \text{s}.$$

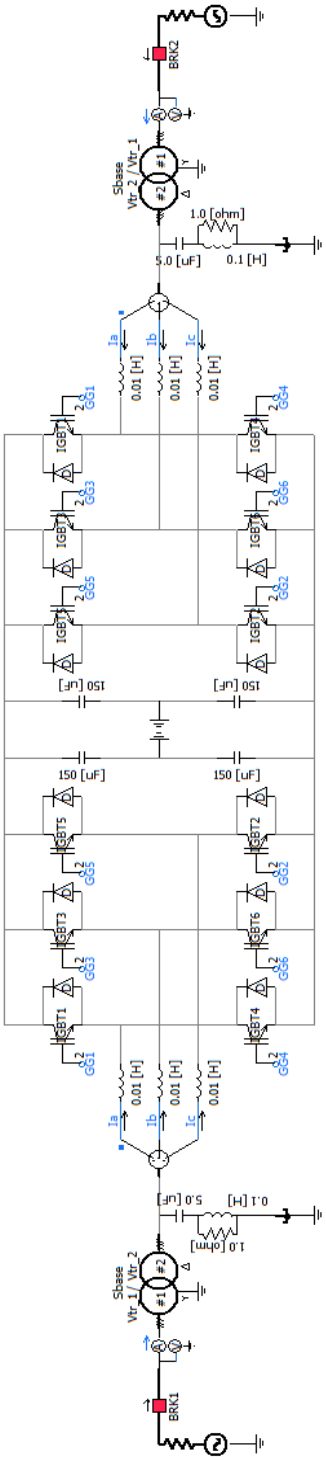

Fig. 14. VSC–HVDC system simulation model built by PSCAD/EMTDC

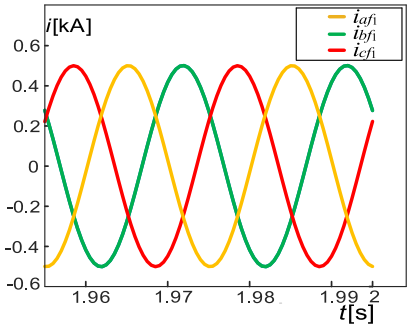

Fig. 15. Three-phase current during normal operation

1) Single-phase grounding of converter transformer valve side bushing

The currents of the grounded a-phase valve-side bushing are shown in Fig. 16(a), and Fig. 16(b) shows the current after the fundamental wave is filtered out. It can be seen that the a-phase current contains a large decaying aperiodic component.

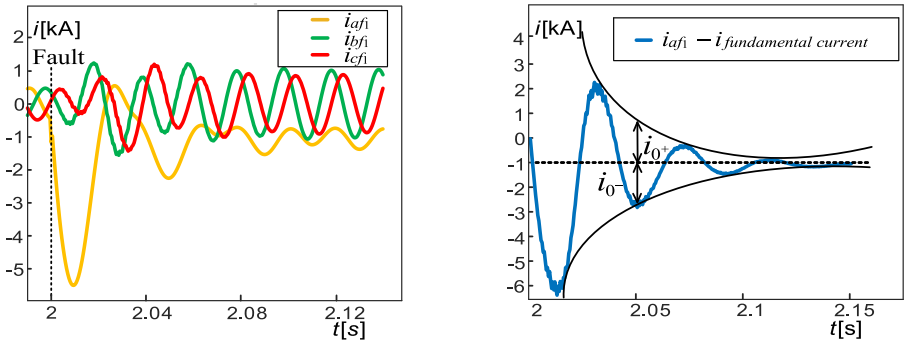

(a) i_{af1}, i_{bf1} and i_{cf1} (b) $i_{af1} - i_{\text{fundamental current}}$

Fig. 16. The simulation results of a-phase grounding of converter transformer valve-side bushing

$t_1 = 2.000$ s and $t_2 = 2.003$ s are respectively selected as the starting points of the half-cycle integral to obtain

$$S_{a\,\text{full current}(t_1)} = 3.527\ \text{A} \cdot \text{s} \quad \text{and} \quad S_{a\,\text{full current}(t_2)} = 7.184\ \text{A} \cdot \text{s}.$$

Then,

$$\left|S_{a\,\text{full current}(t_2)} - S_{a\,\text{full current}(t_1)}\right| = 7.184 - 3.527 = 3.657\ \text{A} \cdot \text{s} > S_{\text{set}}\,. \tag{2}$$

Because $|S_{\Delta\text{full current}}| > S_{\text{set}}$, the blocking criterion is satisfied to block the overcurrent protection.

The simulation result of a-phase grounding with fault resistance $R_f = 100\ \Omega$ on the valve side bushing of the converter transformer is added, and the corresponding three-phase currents and

the current after filtering out the fundamental frequency wave are shown in Fig. 17. Compared to a-phase metallic grounding, the fault phase current decreases but contains the decaying aperiodic component. Select $t_1 = 2.000$ s and $t_2 = 2.003\,A$ as the starting points, respectively, to get the half-cycle integrals as follows:

$$S_{a\,\text{full current}(t_1)} = 3.273\ \text{A}\cdot\text{s} \quad \text{and} \quad S_{a\,\text{full current}(t_2)} = 4.368\ \text{A}\cdot\text{s}.$$

So,

$$\left|S_{a\,\text{full current}(t_2)} - S_{a\,\text{full current}(t_1)}\right| = 4.368 - 3.273 = 1.095\ \text{A}\cdot\text{s} > S_{\text{set}}\,. \tag{3}$$

Therefore, the blocking criterion can still operate to prevent the maloperation of commutation reactance overcurrent protection.

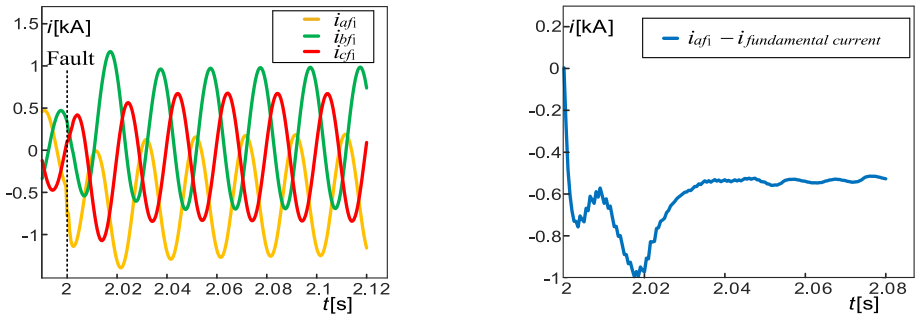

(a) Currents of commutation reactance

(b) Fault phase current after filtering out fundamental wave

Fig. 17. A-phase grounding with fault resistance $R_f = 100\ \Omega$ on the valve side bushing

2) Two-phase short-circuit of converter transformer valve-side bushing

The currents of the a-phase-to-b-phase short circuit that occurs on the valve-side bushing are shown in Fig. 18(a), and Fig. 18(b) shows the currents of the two fault phases after the fundamental wave is filtered out, both of which contain the decaying aperiodic component.

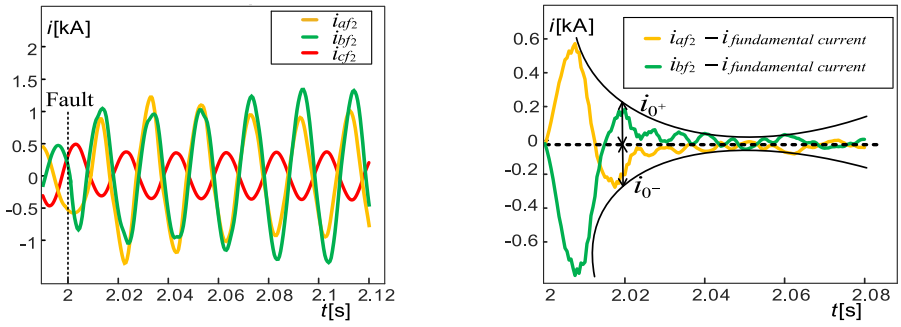

(a) i_{af_2}, i_{bf_2} and i_{cf_2}

(b) $i_{af_2} - i_{\text{fundamental current}}$ and $i_{bf_2} - i_{\text{fundamental current}}$

Fig. 18. The simulation result of two-phase short-circuit of converter transformer valve-side bushing

Select $t_1 = 2.000$ s and $t_2 = 2.003$ s as the starting points, respectively, to get the half-cycle integrals as follows:

$$S_{a\,\text{full current}(t_1)} = 4.178\ \text{A} \cdot \text{s},$$
$$S_{a\,\text{full current}(t_2)} = 5.182\ \text{A} \cdot \text{s},$$
$$S_{b\,\text{full current}(t_1)} = 4.019\ \text{A} \cdot \text{s}$$

and

$$S_{b\,\text{full current}(t_2)} = 5.028\ \text{A} \cdot \text{s}.$$

So,

$$\left|S_{a\,\text{full current}(t_2)} - S_{a\,\text{full current}(t_1)}\right| = 5.182 - 4.178 = 1.004\ \text{A} \cdot \text{s} > S_{\text{set}}\,, \tag{4}$$
$$\left|S_{b\,\text{full current}(t_2)} - S_{b\,\text{full current}(t_1)}\right| = 5.028 - 4.019 = 1.009\ \text{A} \cdot \text{s} > S_{\text{set}}\,. \tag{5}$$

Therefore, the blocking criteria is satisfied, and the overcurrent protection of the corresponding phase will be blocked.

3) Internal grounding of commutation reactance

Figure 19(a) shows the currents of the a-phase grounding of the commutation reactance outlet. The fault-phase current increases, but the decaying aperiodic component is small and has a short existence time.

$$S_{a\,\text{full current}(t_1)} = 3.017\ \text{A} \cdot \text{s} \quad \text{and} \quad S_{a\,\text{full current}(t_2)} = 2.963\ \text{A} \cdot \text{s}.$$

Then,

$$\left|S_{a\,\text{full current}(t_2)} - S_{a\,\text{full current}(t_1)}\right| = 3.017 - 2.963 = 0.054\ \text{A} \cdot \text{s} < S_{\text{set}}\,. \tag{6}$$

The blocking criterion is not satisfied and the overcurrent protection can act.

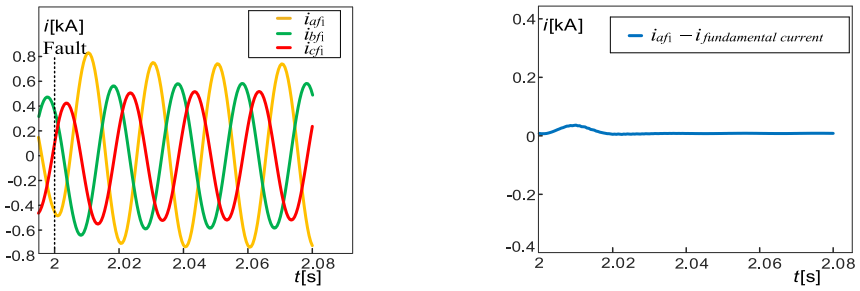

(a) i_{af_1}, i_{bf_1} and i_{cf_1} (b) $i_{af_1} - i_{\text{fundamental current}}$

Fig. 19. The simulation result of a-phase grounding of commutation reactance outlet

4) Internal two-phase short-circuit of commutation reactance

The CT currents after the a-phase-to-b-phase short circuit of the commutation reactance outlet occurs are shown in Fig. 20. The fundamental current of two fault phases increases obviously, but does not contain the attenuated aperiodic component.

$$S_{a\,\text{full current}(t_1)} = 3.012\ \text{A} \cdot \text{s},$$
$$S_{a\,\text{full current}(t_2)} = 3.004\ \text{A} \cdot \text{s},$$

$$S_{b\,\text{full current}(t_1)} = 3.018\ \text{A}\cdot\text{s} \quad \text{and} \quad S_{b\,\text{full current}(t_2)} = 3.024\ \text{A}\cdot\text{s}.$$

So,

$$\left|S_{a\,\text{full current}(t_2)} - S_{a\,\text{full current}(t_1)}\right| = 3.012 - 3.004 = 0.008\ \text{A}\cdot\text{s} < S_{\text{set}}\,, \tag{7}$$

$$\left|S_{b\,\text{full current}(t_2)} - S_{b\,\text{full current}(t_1)}\right| = 3.024 - 3.018 = 0.006\ \text{A}\cdot\text{s} < S_{\text{set}}\,. \tag{8}$$

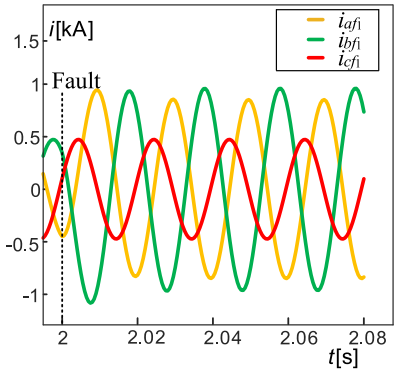

Fig. 20. The simulation result of two-phase short-circuit of commutation reactance outlet

It can be seen that the blocking criteria is not satisfied, and the fault can be removed because the overcurrent protection is not blocked.

In the Fig. 21, the simulation results of blocking criteria under the conditions of the fault on the valve-side bushing of the converter transformer and the fault on commutation reactance are merged in one figure.

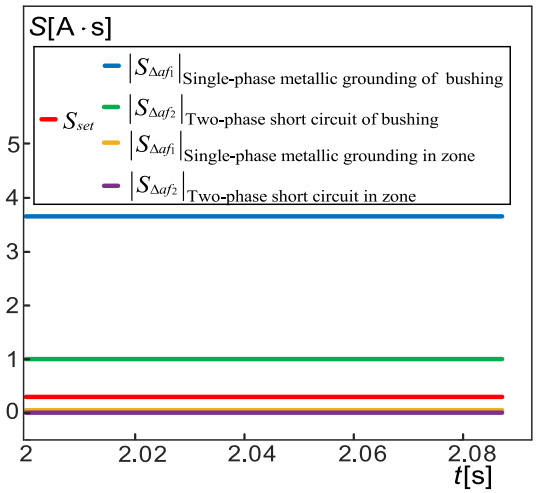

Fig. 21. Simulation results of blocking criteria under different fault conditions

As can be seen from Fig. 21, when a fault occurs on the valve-side bushing, $\left|S_{a(t_2)} - S_{a(t_1)}\right| > S_{\text{set}}$, so the blocking criterion in this paper operates reliably to block the maloperation of overcurrent protection; when a fault occurs on commutation reactance, $\left|S_{a(t_2)} - S_{a(t_1)}\right| < S_{\text{set}}$, therefore, the criterion does not operate and does not block the correct operation of the overcurrent protection.

5. Conclusion

1. When an asymmetric fault occurs on the valve-side bushing of the converter transformer in the VSC–HVDC system because the existence of the fault point reduces the impedance of the AC circuit, the fundamental frequency current flowing through the commutation reactance current transformer is far greater than that during normal operation, which can lead to maloperation of commutation reactance overcurrent protection.

2. Based on the characteristics that the current flowing through the commutation reactance after an asymmetric fault occurs on the valve-side bushing of the converter transformer contains decaying aperiodic components besides the fundamental frequency wave, this paper proposes a scheme to prevent the maloperation of the commutation reactance overcurrent protection. In this scheme, the half-cycle absolute value of the commutation reactance current is integrated, and the inequality of two half cycle integral values with different starting points is utilized to block the maloperation of the protection. The simulation results show that the scheme can reliably block the overcurrent protection when an asymmetric fault occurs on the valve-side bushing of the converter transformer, but does not affect the correct operation of the overcurrent protection when the fault occurs on the commutation reactance.

References

[1] Congshan L., Yikai L., Jian G., Ping H., *Research on emergency DC power support coordinated control for hybrid multi-infeed HVDC system*, Archives of Electrical Engineering, vol. 69, no. 1, pp. 5–21 (2020), DOI: 10.24425/aee.2020.131755.

[2] Yanxia Z., Anlu B., Jian W., Fuhe Z., Jingyi L., *VSC–HVDC transmission line fault location based on transient characteristics*, Archives of Electrical Engineering, vol. 70, no. 2, pp. 381–398 (2021), DOI: 10.24425/aee.2021.136991.

[3] Congshan L., Zikai Z., Tingyu S., Yan L., Pu Z., Xiaowei Z., *Research on influencing factors of emergency power support for voltage source converter-based multi-terminal high-voltage direct current transmission system*, Archives of Electrical Engineering, vol. 71, no. 4, pp. 881–894 (2022), DOI: 10.24425/aee.2022.142114.

[4] Zheng X., Hairong C., *Review and Applications of VSC HVDC*, High Voltage Engineering, vol. 33, no. 1, pp. 1–10 (2007), DOI: 10.13336/j.1003-6520.hve.2007.01.001.

[5] Hongtao J., Yinghong L., Yuheng F., Shengxiong P., *Improved carrier phase shift modulation and voltage equalization control strategy in modular multilevel converter*, Archives of Electrical Engineering, vol. 68, no. 4, pp. 803–815 (2019), DOI: 10.24425/aee.2019.130684.

[6] Guangfu T., Zhiyuan H., Hui P., *Research, Application, and Development of VSC–HVDC Engineering Technology*, Automation of Electric Power Systems, vol. 37, no. 15, pp. 3–14 (2013), DOI: 10.7500/AEPS20130224003.

[7] Yibo G., Xidong X., Yangxin J., *Impact on the Voltage Balancing of DC Distribution Network Under AC Side Grounding Fault*, Power System Technology, vol. 38, no. 10, pp. 2665–2670 (2014), DOI: 10.13335/j.1000-3673.pst.2014.10.008.

[8] Guozheng L., Liang G., Zhimin L., *Influence of voltage source converter grounding mode on DC distribution system*, Power System Protection and Control, vol. 44, no. 12, pp. 75–80 (2016), DOI: 10.7667/PSPC151252.

[9] Jie Y., Jianchao Z., Guangfu T., Zhiyuan H., *Grounding Design Analysis of VSC–HVDC System*, Proceedings of the CSEE, vol. 30, no. 19, pp. 0014–0019 (2010), DOI: 10.13334/j.0258-8013.pcsee.2010.19.014.

[10] Jie Y., Jianchao Z., Guangfu T., Zhiyuan H., *Internal AC Bus Fault Characteristics of VSC–HVDC System and Protection Coordination*, Proceedings of the CSEE, vol. 30, no. 16, pp. 0006–0011 (2010), DOI: 10.13334/j.0258-8013.pcsee.2010.16.001.

[11] Juanjuan W., *Simulation and analysis of VSC–HVDC system failure*, PhD Thesis, Mechanical and Electronic Engineering, Xi'an University of Architecture and Technology, Xi'an (2015).

[12] Xiaoyun S., Xin G., Xiangqian T., *Fault diagnosis algorithm for converter of VSC–HVDC system with failed valve arm blocking*, Electric Power Automation Equipment, vol. 38, no. 10, pp. 121–126 (2018), DOI: 10.16081/j.issn.1006-6047.2018.10.019.

[13] Guanming Z., Chunju F., Linyue Q., Jianjun S., Shumin S., Guanglei L., *Response Characteristics of AC Bus Fault in Converter Station of VSC-based DC Distribution Network*, Proceedings of the CSU-EPSA, vol. 31, no. 1, pp. 132–141 (2019), DOI: 10. 3969/j. issn. 1003-8930. 2019. 01. 021.

[14] Guangfu T., *High-voltage DC transmission technology based on voltage source converters*, China Electric Power Press (2009).

[15] Guanqian J., Zhiyong L., Huixia Y., Jing Y., *Research review on topological structure of flexible HVDC system*, Power System Protection and Control, vol. 43, no. 15, pp. 145–153 (2015), DOI: JournalArticle/5b3beda4c095d70f00991a7e.

[16] Zhiqing Y., Fei Y., Qian Z., Qun Z., *Simulation Research on Large-scale PV Grid-connected Systems Based on MMC*, Proceedings of the CSEE, vol. 33, no. 36, pp. 27–33 (2013), DOI: 10.13334/j.0258-8013.pcsee.2013.36.009.

[17] Guangfu T., Xiang L., Xiaoguang W., *Multi-terminal HVDC and DC-grid Technology*, Proceedings of the CSEE, vol. 33, no. 10, pp. 8–17 (2013), DOI: 10.13334/j.0258-8013.pcsee.2013.10.002.

[18] Yanxia Z., Yue H., Yachao C., Kaixiang L., *Fault Analysis for Valve Side Winding of Converter Transformer*, Power System Technology, vol. 46, no. 07, pp. 2794–2803 (2022), DOI: 10.13335/j.1000-3673.pst.2021.1492.

[19] Rui Q., Fubo L., Yong Z., Lixin C., *Analysis of VSC–HVDC Distribution System Modeling and Fault Transient*, Smart Grid, vol. 3, no. 12, pp. 1143–1148 (2015), DOI: 10.14171/j.2095-5944.sg.2015.12.010.